AN IMPROVED MODEL FOR RELATIVE PERMEABILITY AND CAPILLARY PRESSURE INCORPORATING WETTABILITY

David. D. Huang, Matt M. Honarpour, and Rafi Al-Hussainy
Mobil Technology Company, 13777 Midway Road, Texas, 75244

This paper is prepared for presentation at the 1997 SCA International Symposium
Calgary, Canada, September 7-10, 1997

Abstract

Pore sizes, pore structures, relative permeability, capillary pressure, and wettability are measured as part of special core analysis. Inconsistency among measurements sometimes occurs because, for example, residual fluid saturations are different in different experiments, and preferential wettability changes during laboratory handling, experimentation, and core restoration. Furthermore, it is expensive to conduct different experiments that duplicate information on the same porous media. This memorandum presents a model that integrates relative permeabilities, capillary pressure, wettability indices, and pore size distribution in a consistent manner.

The model has the potential to be used in reservoir simulations to populate unmeasured rock-fluid properties based on limited measurements. It can be used for relative permeability and capillary pressure scaling up. In near future, we will fine-tune the model with measurements and published data. We will then extend the model to incorporate lithological data and core-level parameters such as absolute permeability, porosity, residual saturations, and end-point permeabilities.

I. Summary of Results

- An integrated model that interrelates relative permeabilities, capillary pressures, wettability indices (USBM and Amott-Harvey), and pore size distribution is presented. The model can be further extended to include water and oil residual saturations.
- The model is being developed for eventual use to populate and predict unmeasured core properties for numerical simulations of reservoir performance, and thus reduce cost for unnecessary measurements. It could also be further developed for predicting effective relative permeability of complex geological systems.

II. Introduction

In order to mathematically model the movement of fluids in a reservoir, functional relationships between relative permeabilities (k_r), capillary pressure (Pc) and saturation (S) must be known. The relationships between k_r-S, k_r-Pc, and Pc-S are commonly obtained from different measurements and they often lack consistency. For example, the values of residual oil saturation (S_{or}) and interstitial water saturation (S_{iw}) obtained from relative permeability measurements often differ from those derived from capillary pressure measurements. It is also known that both k_r and Pc exhibit hysteresis, but the fact that k_r-hysteresis must interrelate with Pc-hysteresis is customarily ignored.

Capillary pressure, relative permeability, their hysteresis phenomena, and residual fluid saturations (S_{or} and S_{iw}) are functions of pore size distribution and wettability. All these factors may be influenced by fluid properties, temperature, and pressure. **Figure 1** shows these interrelationships.

The top three elements in **Figure 1** (fluid properties, rock properties, and temperature and pressure) are reservoir-specific (i.e., rock-type specific). The purpose of this paper is therefore to develop a core-level model that interrelates capillary pressure and relative permeabilities with pore size distribution and wettability in a consistent manner. Such a model is lacking in the industry, and the development of the model is needed because unmeasured core properties could be predicted from a certain set of measured properties using the model.

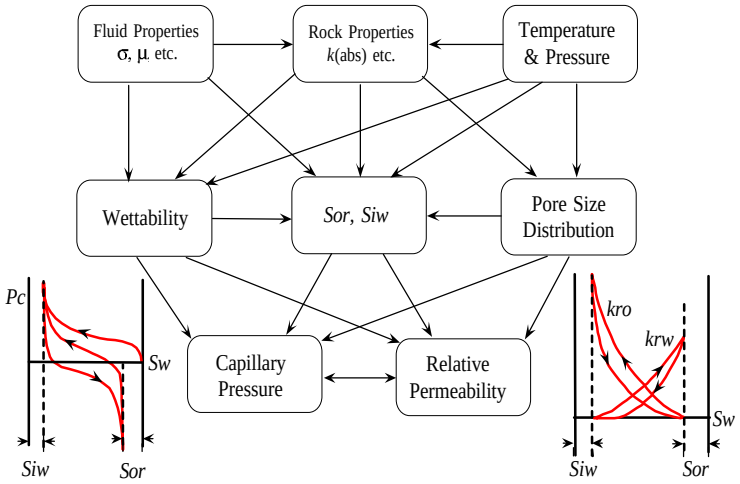

Figure 1. Inter-relationship among rock-fluid properties: capillary pressure, relative permeability, pore size distribution, wettability, and residual saturations.

We now review and discuss previous works which are building blocks of a model that we have constructed:

(a) The Capillary Pressure (*Pc*) - Relative Permeability (k_r) Relationships

Capillary pressure and relative permeability relationships have long been derived based on the Kozeny equation[1] and the bundle-of-capillary-tube model[2] with tortuosity[3] and/or electric resistivity[4,5] accounted. The classical Corey-Burdine[6,7,8] equations relate *Pc* and k_r of a porous media without linking wettability and pore size distribution. There are a few other *Pc*-k_r relationships that are less popular than the Corey-Burdine formulation: the Rapoport-Leas model[9] and the Mualem model[10]; the latter is believed to be more applicable to unconsolidated cores and soil packs[11,12]. Using the Corey-Burdine equations, Corey[6,8] prescribed a power-law form for *primary drainage* capillary pressure to calculate drainage k_r.

Naar and Henderson[13] proposed a model that uses the *primary drainage* capillary pressure to calculate k_r in the *primary imbibition* direction (see Eqs. (30)-(32) of ref. 13). Similarly, Land[14,15] used the *primary drainage Pc* curve and the Corey-Burdine equations to calculate *primary imbibition* k_r. The Land theory has somewhat been standardized[16], and its applications were published recently[17,18]. However, these works are not theoretically rigorous because *imbibition* k_r *should be calculated based on imbibition Pc*.

(b) Pore Size Distribution - Capillary Pressure (*Pc*) Relationships

Capillary pressures are commonly measured by porous diaphragm method[19], mercury-injection method[2,20], and centrifuge method[21]. *Pore size distribution* is traditionally inferred from the mer-

cury-injection *primary intrusion Pc* data[22] through the Young-Laplace equation because mercury is strongly nonwetting. The volume of mercury injected for a given pressure increment represents the combined volume of (pore-)throats and (pore-)bodies that are connected by throats falling within specific size limits. However, not all bodies and throats within the specific size range can be invaded by mercury, because they may be shielded by other smaller pores whose displacement pressure has not yet been exceeded. Such effects can be studied conveniently by constructing idealized pore models[23,24,25]. These studies found that throats and throat-to-body accessibility control the entry pressure. Thus, capillary pressure curve may differ quite significantly from actual throat size distribution. If withdrawal of mercury (i.e., wetting-phase imbibition process) is mainly from "throats" rather than "bodies," then withdrawal volume can be used as a measure of "throat" volume and, by subtraction from total void volume, "body" volume also can be estimated.

(c) Capillary Pressure (*Pc*) - Saturation (*S*) Relationships

Corey[6,8] used a power-law form for primary drainage capillary pressure. Van Genuchten[11] used another three-parameter function for primary drainage *Pc*. Identical functional form was used to represent primary imbibition *Pc* by Parker and Lenhard[26]. All these *Pc* representations involve curve-fitting fudge factors, and are not directly associated with pore size distribution and/or "fluid size distribution."

(d) Wettability - Capillary Pressure (*Pc*) Relationships

Capillary pressure behavior is related to the wettability of the core[27]. The so-called USBM and Amott-Harvey Indices[28,29] are calculated based on to the primary imbibition (or secondary imbibition) and secondary drainage *Pc* curves.

Based on the above discussions, this paper will provide a first-pass attempt to integrate capillary pressure, relative permeabilities, hysteresis, pore size distribution, and wettability in a consistent manner. The development of the model is presented in the next section.

III. Model Development

(a) Log-Normal Distribution for Free Pore Space

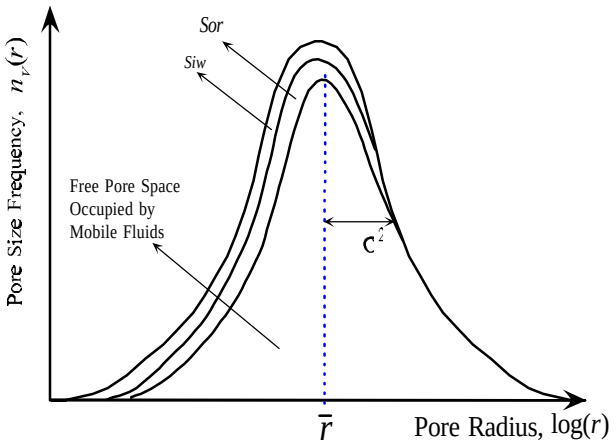

Figure 2. Log-normal pore/throat size distribution for free pore spaces.

In most intergranular reservoir rocks, the pore space occupied by mobile fluids, which we will call "*free pore volume*," may be approximated by a *log-normal* distribution[30]. There are some other representations of pore size distribution, such as the Gamma

distribution[31], but the mathematics becomes more cumbersome than what is presented in this paper. In future efforts, we will fine-tune the present model with some measured parameters, and will improve the approximate nature of the log-normal distribution. A log-normal distribution is a Gaussian distribution with its independent variable (i.e., the pore/throat size) in logarithmic scale and the dependent variable (i.e., the pore frequency) in linear scale. Denoting $n_V(r)$ as the frequency of pore/throat sizes of the free pore volume, a hypothetical log-normal distribution of $n_V(r)$ is shown in **Figure 2**.

$n_V(r)$ is represented by Equation (1), in which r is the equivalent pore/throat radius, $\bar{r}$ is the volume-median pore/throat radius, and σ is the standard deviation:

$$n_V(r) = \frac{V_{\text{Free}}}{\sqrt{2\pi}\, r \ln\sigma} \exp\left[-\ln^2\left(\frac{r}{\bar{r}}\right) \Big/ 2\ln^2\sigma\right] \tag{1}$$

V_{Free} is the total free pore volume, and is equal to the integration of $n_V(r)$ over the entire r domain (r = 0 to ❄):

$$\int_0^{\infty} n_V(r)\, dr = V_{\text{Free}} \tag{2}$$

The $\bar{r}$ in Eq. (1) is the radius below which the area under the $n_V(r)$ vs. r curve is one-half of V_{Free}, this explains why $\bar{r}$ is called the *volume-median* pore/throat radius:

$$\int_0^{\bar{r}} n_V(r)\, dr = \frac{1}{2} V_{\text{Free}} \tag{3}$$

Using Eq. (1), $n_V(r)$ function can be integrated with respect to r from r = 0 to an arbitrary pore/throat size r to give:

$$V(r) = \int_0^r n_V(r)\, dr = \frac{1}{2} V_{\text{Free}} \left[1 + \text{erf}\left(\ln\frac{r}{\bar{r}} \Big/ \sqrt{2}\ln\sigma\right)\right] \tag{4}$$

where $V(r)$ is the "partial" free pore volume occupied by a phase from the smallest pore (r=0) to an arbitrary pore size r. Eq. (4) is important in a sense that it gives a relationship between *normalized phase saturation* and *capillary pressure.* "Normalized saturation" (S^*) is the ratio of the partial free pore volume divided by the total free pore volume:

$$S^* = \frac{V(r)}{V_{\text{Free}}} \tag{5}$$

The capillary pressure (P_c) is related to the pore/throat radius by the Young-Laplace equation:

$$\left|P_c\right| = \frac{2\gamma\cos\theta}{r}; \qquad \left|\bar{P}_c\right| = \frac{2\gamma\cos\theta}{\bar{r}} \tag{6a, 6b}$$

where γ is the interfacial tension between phases, θ is the rock-fluid contact angle, and $\bar{P}_c$ is the capillary pressure corresponding to the volume-median pore/throat radius, $\bar{r}$. Eq. (4) therefore can be written in the following form:

$$S^* = \frac{1}{2}\left[1 + \text{erf}\left(\ln\frac{\bar{P}_c}{P_c} \Big/ \sqrt{2}\ln\sigma\right)\right] \tag{7}$$

This equation represents a simplified relationship between S^* and Pc. Similar expressions for Pc in the primary imbibition and secondary drainage directions will be derived in the next section based on Eq. (7).

(b) Capillary Pressure (P_c) - Saturation (S_w^*) Relationship for Primary Imbibition and Secondary Drainage

A schematic representation of capillary pressure behavior during repeated drainage (oilflood) and imbibition (waterflood) cycles is shown in **Figure 3**. In this figure, the *x*-axis is un-normalized water saturation. Left and right arrows show water drainage and imbibition, respectively. Segment 1 is primary water drainage, Segments 2 and 3 together account for primary water imbibition, and Segments 4 and 5 together represent secondary water drainage. Segments 2 and 4 are spontaneous water imbibition and oil imbibition, respectively. Segments 3 and 5 are forced water drive and forced oil drive, respectively.

The two quantities, *X* and *Y*, shown in **Figure 3** are related to the wettability of the system. *X* represents how much water can be automatically imbibed by the rock without putting any pressure gradient. *Y*, similarly, represents spontaneous oil imbibition. Later as we will show, the two commonly used USBM and Amott-Harvey wettability indices can be related to *X* and *Y*.

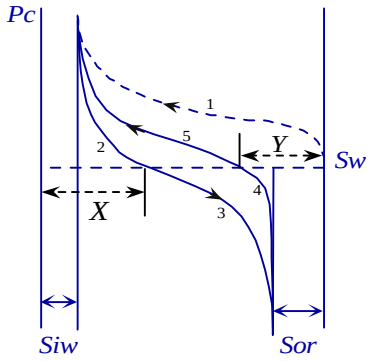

Figure 3. A graphical representation of capillary pressures as functions of water saturation in a water-oil system. Segment (1): primary water drainage; Segment (2): spontaneous water imbibition; Segment (3): forced water imbibition (or water drive); Segment (4): spontaneous water drainage; and Segment (5): forced water drainage (or oil drive).

In **Figure 3**, primary imbibition and secondary drainage are enclosed within a saturation of range 1 - S_{iw} - S_{or}, which corresponds to the pore space occupied by mobile fluids only (i.e., excluding connate water and residual oil). The water saturation S_w can be thus normalized:

$$S_w^* = \frac{S_w - S_{iw}}{1 - S_{iw} - S_{or}} \tag{8}$$

The extent of spontaneous water and oil imbibition, *X* and *Y*, can as well be normalized as:

$$X^* = \frac{X - S_{iw}}{1 - S_{iw} - S_{or}} \;; \quad Y^* = \frac{Y - S_{or}}{1 - S_{iw} - S_{or}} \tag{9a,b}$$

To a first approximation, we assume that in each of Segments 2, 3, 4, and 5, water imbibes or drains into pore/throat sizes that are always log-normally distributed, and each segment has one log-normal distribution function of its own. We further assume that these four log-normal distribution functions (of Segments 2, 3, 4, and 5) have same mean pore/throat size and standard deviation. Therefore, similar to the derivation of Eq. (7), we have the following equations relating S_w^* with P_c for each segment:

(Segment 2): Spontaneous Water Imbibition:

$$S_w^* = \frac{1}{2} X^* \left[1 + \mathrm{erf}\left(\ln \frac{\overline{P}_c}{P_c} \Big/ \sqrt{2} \ln \sigma \right) \right] \tag{10}$$

(Segment 3): Forced Water Imbibition (or Water Drive):

$$S_w^* = 1 - \frac{1}{2}(1 - X^*)\left[1 + \text{erf}\left(\ln\left(-\frac{\overline{P}_c}{P_c}\right)\Big/\sqrt{2}\ln\sigma\right)\right] \tag{11}$$

(Segment 4): Spontaneous Water Drainage (or Spontaneous Oil Imbibition):

$$S_w^* = 1 - \frac{1}{2}Y^*\left[1 + \text{erf}\left(\ln\left(-\frac{\overline{P}_c}{P_c}\right)\Big/\sqrt{2}\ln\sigma\right)\right] \tag{12}$$

(Segment 5): Forced Water Drainage (or Oil Drive):

$$S_w^* = \frac{1}{2}(1 - Y^*)\left[1 + \text{erf}\left(\ln\frac{\overline{P}_c}{P_c}\Big/\sqrt{2}\ln\sigma\right)\right] \tag{13}$$

(c) Wettability Indices Derived from the Capillary Pressure (*Pc*) - Saturation (S_w^*) Relationship

With the P_c-saturation relationships given by Eqs. (10)-(13), the conventional USBM and Amott-Harvey wettability indices can be derived as follows:

Amott-Harvey Wettability Index **(I_{AH}):**

Amott-Harvey index is defined as the spontaneous amount of water imbibition minus that of spontaneous oil imbibition.

$$I_{AH} = \frac{X - S_{iw}}{1 - S_{iw} - S_{or}} - \frac{Y - S_{or}}{1 - S_{iw} - S_{or}} = X^* - Y^* \tag{14}$$

The physical significance of Amott-Harvey is apparent from Eq. (14): the greater the spontaneous water imbibition, the larger the value of X^*, and the closer I_{AH} to unity. So, I_{AH} = 1 represents perfectly water-wetting characteristic. Similarly, I_{AH} = -1 represents perfectly oil-wetting characteristic. However, any intermediate value of I_{AH} between -1 and 1 could mean that the system is both water-wetting and oil-wetting (e.g., X^* = 0.3 and Y^* = 0.3 gives I_{AH} = 0), or it could mean that the system is non-wetting to both phases (e.g., X^* = 0 and Y^* = 0 also gives I_{AH} = 0).

USBM Wettability Index **(I_{USBM}):**

The USBM index is defined as the logarithmic of the ratio of the *energy* required for forced water drainage to the *energy* required for forced oil drainage. *Energy* is equal to the product of capillary pressure and the pore volume, so,

$$\text{Energy required for forced water drainage} = V_{\text{Free}}\int_0^{1-Y^*} P_c\, dS^* = V_{\text{Free}}\, A_1 \tag{15}$$

and $$\text{Energy required for forced oil drainage} = V_{\text{Free}}\int_{X^*}^{1} (-P_c)\, dS^* = V_{\text{Free}}\, A_2 \tag{16}$$

In Eqs. (15) and (16), A_1 is the area enclosed by the positive capillary pressure curve of Segment 5 and the S_w-axis as shown in **Figure 3**. A_2 is the area enclosed by the negative capillary pressure curve of Segment 3 and the S_w-axis. With these expressions, USBM index is commonly written in the form:

$$I_{USBM} = \log_{10}(A_1/A_2) \tag{17}$$

Eq. (11) for Segment 3 and Eq. (13) for Segment 5 now can be used to calculate A_1 and A_2. The results of integration are:

$$A_1 = \int_0^{1-Y^*} P_c\big|_{\text{step 5}}\, dS_w^* = (1-Y^*)\,\overline{P}_c\ \exp\left(\frac{1}{2}\ln^2\sigma\right) \tag{18}$$

$$A_2 = \int_{X^*}^{1} (-P_c)\big|_{\text{step 3}}\, dS_w^* = (1-X^*)\,\overline{P}_c\ \exp\left(\frac{1}{2}\ln^2\sigma\right) \tag{19}$$

Subsequently, the USBM index is: $I_{USBM} = \log_{10}\left(\dfrac{1-Y^*}{1-X^*}\right)$ (20)

Unlike the Amott-Harvey index, the USBM index can have values greater than unity or smaller than -1. Also, from the comparison of Eq. (14) of I_{AH} and Eq. (20) of I_{USBM}, we see that there is no direct one-to-one relationship between these two indices.

(d) Interrelationship of Capillary Pressure (P_c) and Relative Permeability (k_r) - The use of Corey-Burdine Equations

The Corey-Burdine equations provide linkages between the capillary pressure and relative permeabilities for both water and oil phases. The equations are:

$$k_{rw} = \left(S_w^*\right)^2 \frac{\displaystyle\int_0^{S_w^*} \frac{1}{(P_c)^2}\, dS_w^*}{\displaystyle\int_0^1 \frac{1}{(P_c)^2}\, dS_w^*} \quad ; \; k_{ro} = \left(1-S_w^*\right)^2 \frac{\displaystyle\int_{S_w^*}^1 \frac{1}{(P_c)^2}\, dS_w^*}{\displaystyle\int_0^1 \frac{1}{(P_c)^2}\, dS_w^*} \tag{21a,b}$$

Calculation of the integrals in Eqs. (21a) and (21b) involves using Eqs. (10) through (13) and change of variables. The final results of the k_{ro} and k_{rw} expressions are:

(Segment 2): Spontaneous Water Imbibition:

$$k_{rw} = \frac{1}{2} X^* \left(S_w^*\right)^2 \left[1 - \text{erf}\left(\sqrt{2}\ln\sigma - \frac{1}{\sqrt{2}\ln\sigma}\ln\frac{\overline{P}_c}{P_c}\right)\right] \tag{22a}$$

$$k_{ro} = \left(1-S_w^*\right)^2 \left\{1 - \frac{1}{2} X^* \left[1 - \text{erf}\left(\sqrt{2}\ln\sigma - \frac{1}{\sqrt{2}\ln\sigma}\ln\frac{\overline{P}_c}{P_c}\right)\right]\right\} \tag{22b}$$

(Segment 3): Forced Water Imbibition (or Water Drive):

$$k_{rw} = \left(S_w^*\right)^2 \left\{1 - \frac{1}{2}(1-X^*)\left[1 - \text{erf}\left(\sqrt{2}\ln\sigma - \frac{1}{\sqrt{2}\ln\sigma}\ln\frac{\overline{P}_c}{(-P_c)}\right)\right]\right\} \tag{23a}$$

$$k_{ro} = \frac{1}{2}(1-X^*)\left(1-S_w^*\right)^2 \left[1 - \text{erf}\left(\sqrt{2}\ln\sigma - \frac{1}{\sqrt{2}\ln\sigma}\ln\frac{\overline{P}_c}{(-P_c)}\right)\right] \tag{23b}$$

(Segment 4): Spontaneous Water Drainage (or Spontaneous Oil Imbibition):

$$k_{rw} = \left(S_w^*\right)^2 \left\{1 - \frac{1}{2} Y^* \left[1 - \text{erf}\left(\sqrt{2}\ln\sigma - \frac{1}{\sqrt{2}\ln\sigma}\ln\frac{\overline{P}_c}{(-P_c)}\right)\right]\right\} \tag{24a}$$

$$k_{ro} = \frac{1}{2} Y^* \left(1 - S_w^*\right)^2 \left[1 - \text{erf}\left(\sqrt{2}\ln\sigma - \frac{1}{\sqrt{2}\ln\sigma}\ln\frac{\overline{P}_c}{(-P_c)}\right)\right] \quad (24b)$$

(Segment 5): Forced Water Drainage (or Oil Drive):

$$k_{rw} = \frac{1}{2}(1 - Y^*)\left(S_w^*\right)^2 \left[1 - \text{erf}\left(\sqrt{2}\ln\sigma - \frac{1}{\sqrt{2}\ln\sigma}\ln\frac{\overline{P}_c}{P_c}\right)\right] \quad (25a)$$

$$k_{ro} = \left(1 - S_w^*\right)^2 \left\{1 - \frac{1}{2}(1 - Y^*)\left[1 - \text{erf}\left(\sqrt{2}\ln\sigma - \frac{1}{\sqrt{2}\ln\sigma}\ln\frac{\overline{P}_c}{P_c}\right)\right]\right\} \quad (25b)$$

IV. Sample Calculations and Model Validation

(a) Sample Calculations

Relative permeability and capillary pressure were calculated for three different wettability conditions. Log-normal distribution was assumed with standard deviation σ = 2.5 and mean $\overline{P}_c$ = 2.5 psi. The predicted P_c and k_r for primary imbibition (dashed lines) and secondary drainage (solid lines) are both shown in **Figure 4**. The top three figures in **Figure 4** are the P_c-S_w^* relationship for the following wetting conditions:

Top Left in **Figure 4**:	I_{USBM} = 0.477,	I_{AH} = 0.6	(X^* = 0.7, Y^* = 0.1)
Top Middle in **Figure 4**:	I_{USBM} = 0.109,	I_{AH} = 0.2	(X^* = 0.3, Y^* = 0.1)
Top Right in **Figure 4**:	I_{USBM} = -0.046,	I_{AH} = -0.1	(X^*=0.0, Y^* = 0.1)

The corresponding relative permeability curves (k_{rw}-S_w^* and k_{ro}-S_w^*) for these cases are shown in the lower half of **Figure 4**. It can be concluded from **Figure 4** that:

1. Hysteresis of relative permeability in both phases is more pronounced when the capillary hysteresis is more significant. The secondary drainage k_{ro} is always higher than the primary imbibition k_{ro} at all saturations. Conversely, the secondary drainage k_{rw} is always lower than the primary imbibition k_{rw} at all saturations.
2. On the basis of the two figures far left, the k_r hysteresis of the wetting phase (water) in more pronounced than the nonwetting phase (oil) in a water-wet system.
3. Based on the three lower figures, the cross point of k_{ro} and k_{rw} in the imbibition direction (dashed lines) moves from the right-hand side (see the lower-left figure) to the left-hand side (see the lower right figure), when wettability condition changes from water-wetting to oil-wetting. This prediction is in agreement with our common observations in measurements[32,33].
4. As long as the capillary curve does not change the cross point of k_{ro}-k_{rw} will not change, even though the wettability changes. This can be exemplified by the secondary drainage calculations (solid lines in **Figure 4**).
5. In the direction of water drainage, even though our calculation focused on in the normalized range of saturation (i.e., S_w^*), water is effectively immobile until S_w^* = 30%. This is also in agreement with common observations in measurements. Similar observation is for the oil phase in the water-imbibition direction; the effective residual oil does not occur at S_w^* = 1 but at about S_w^* = 75%. These observations agree with the fact that k_{ro} at low oil saturation and k_{rw} at low water saturation are very difficult to measure in standard laboratory experiments.

(b) Model Validation with Measured Data

In the published literature, simultaneous measurements of relative permeability and capillary pressure were attempted[34,35], but very accurate and reliable data in both primary imbibition and secondary drainage directions are rare[36]. We found a data set[37] suitable for validation of our modeling based on measurements on a 260-mD fired Berea core sample. The original relative permeability data are adjusted to match end-point relative permeabilities from the predictions: k_{ro} = 0.58 @ S_{iw} = 0.242 and k_{rw} = 0.55 @ S_{or} = 0.274, and the adjusted data is shown in **Table 1**. The reason for this adjustment is that the lab-measured values of S_{iw} (33.9%) and S_{or} (37.1%) are not representative of the true residual saturations which we estimated as S_{iw} = 24.2% and S_{or} = 27.4%.

Table 1. Summary of Relative Permeability Data (Measured at NIPER)

Normlz'd Water Saturation, S_w^*	k_{ro} Imbibition	k_{rw} Imbibition	Normlz'd Water Saturation, S_w^*	k_{ro} Drainage	k_{rw} Drainage
0.2004	0.5800	0	0.7955	0.0008	0.5365
0.4493	0.3457	0.1283	0.7810	0.00414	0.5263
0.4824	0.2105	0.2022	0.7748	0.01964	0.4513
0.6045	0.1397	0.2847	0.6591	0.0525	0.3338
0.6777	0.0200	0.4303	0.5723	0.1109	0.1887
0.7355	0.00416	0.5344	0.4917	0.1760	0.1671
0.7996	0	0.55	0.4462	0.2218	0.1240
			0.3409	0.4120	0
			0.2004	0.58	0

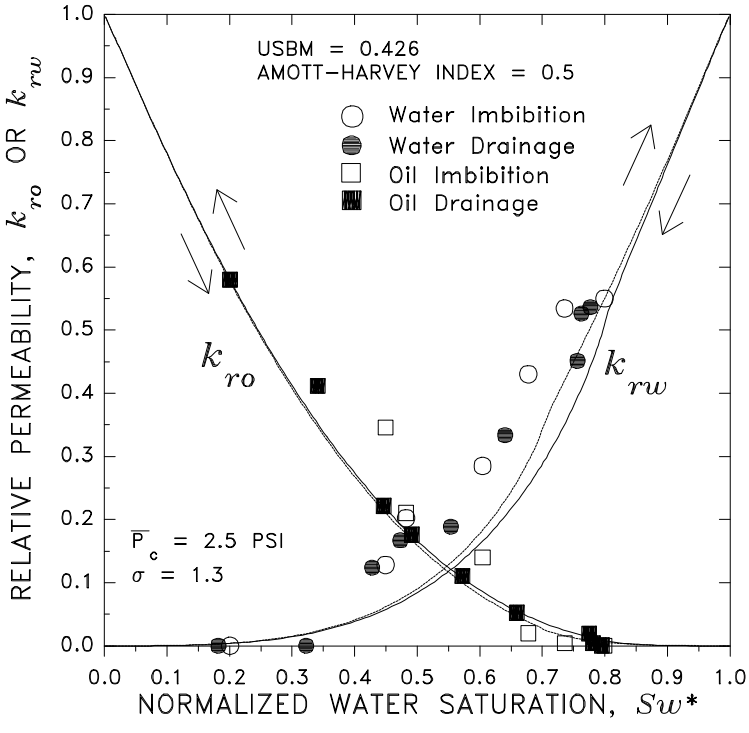

Figure 5. Water-oil relative permeability model-data comparison.

Using the measure log-normal parameters for pore size distribution (σ = 1.3, and $\overline{P}_c$ = 2.5 psi), relative permeability was predicted and compared with measured data as shown in **Figure 5**. The measured k_{rw} for water drainage is always lower than that of the imbibition process, which is in agreement with the predictions. The measured and predicted cross points of k_{ro} and k_{rw} are also well matched with each other. The comparisons of the capillary pressure curves are not shown due to lack of data.

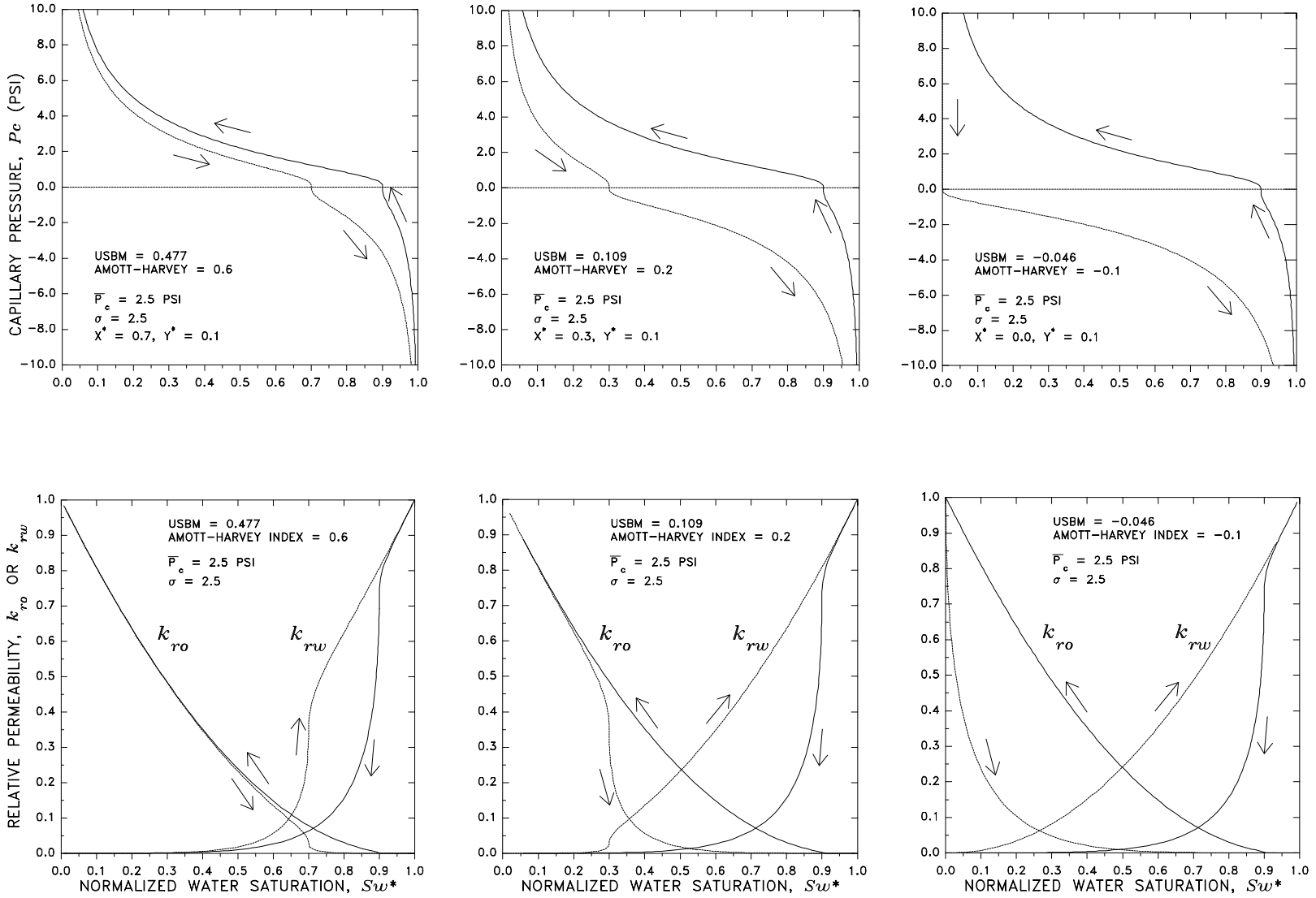

Figure 4. Predicted capillary pressure and relative permeability relationship at different wettability conditions: USBM = 0.477 (left two figures), USBM = 0.109 (middle two figures), USBM = -0.046 (right two figures).

V. Impact and Future Research Directions

Using the model as a first pass, we are able to predict unmeasured core properties from limited measurements, thus reduce cost by avoiding unnecessary measurements. Further, even though the interpretation of the proposed model is based on a water-oil 2-phase system, the model could be extended to predict the k_r-P_c-wettability relationships for gas-oil and gas-water 2-phase systems as well as 3-phase systems. It may have direct application on complex processes such as WAG and gas condensate.

The developed model will still need to be improved and fined-tuned with the use of measured data. The future research areas based on the current developed model could be the following:

- capillary pressure and relative permeability hysteresis behavior at different wettability conditions targeting the differences between mixed-wet and intermediate-wet systems;
- pore size distribution vs. fluid size distribution and their correlations with the model;
- correlations between residual saturations (S_{iw} and S_{or}) and end-point relative permeabilities (k_{ro} @ S_{iw} and k_{rw} @ S_{or});
- scaling lab-measured k_r and P_c to field values of S_{iw} (i.e., different S_{iw} effect); and
- interfacial tension variation and its influence to capillary pressure and relative permeability.

VI. Acknowledgments

We thank Mobil management for approval of publication of this paper.

VII. Reference

[1] Wyllie, M. R. J., and Gardner, G. H. F., "The Generalized Kozeny-Carman Equation - Part 1& 2," World Oil, Production Section, March 121-128 ; April 210-228 (1958).

[2] Purcell, W. R., "Capillary Pressures - Their Measurement Using Mercury and the Calculation of Permeability Therefrom," Trans. AIME **186**, February 39-48 (1949).

[3] Fatt, I., and Dykstra, H., "Relative Permeability Studies," Trans. AIME **192**, 249-256 (1951).

[4] Rose, W., and Wyllie, M. R. J., "A Note on the Theoretical Description of Wetting Liquid Relative Permeability Data," Trans. AIME, December p.329 (1949).

[5] Wyllie, M. R. J., and Spangler, M. B., "Application of Electrical Resistivity Measurements to Problem of Fluid Flow in Porous Media," Bull. AAPG **36**, 359-403 (1952).

[6] Corey, A. T., "The Interrelation Between Gas and Oil Relative Permeability," Producers Monthly, November 38-41 (1954).

[7] Burdine, N. T., "Relative Permeability Calculations from Pore Size Distribution Data," Trans. AIME **198**, 71-78 (1953).

[8] Brooks, R. H., and Corey, A. T., "Hydraulic Properties of Porous Media," Hydrology Papers No. 3, Colorado State University, March 1964.

[9] Rapoport, L. A., and Leas, W. J., "Relative Permeability to Liquid in Liquid-Gas Systems," Trans. AIME **192**, 83-98 (1951).

[10] Mualem Y., "A New Model for Predicting the Hydraulic Conductivity of Unsaturated Porous Media," Water Resources Research **12**, June 513-521 (1976).

[11] Van Genuchten, M. T., "A Closed-form Equation for Predicting the Hydraulic Conductivity of Unsaturated Soils," Soil Sci. Soc. Am. J. **44**, 892-898 (1980).

[12] Lenhard, R. J., and Parker, J. C., "A Model for Hysteretic Constitutive Relations Governing Multiphase Flow, 2. Permeability-Saturation Relations," Water Resources Research **23**, 2197-2206 (1987).

[13] Naar, J., and Henderson, J. H., "An Imbibition Model - Its Application to Flow Behavior and the Prediction of Oil Recovery," Trans. AIME **222**, 61-70 (1961).

[14] Land, C. S., "Calculation of Imbibition Relative Permeability for Two- and Three-Phase Flow From Rock Properties," SPEJ, June 149-156 (1968).
[15] Land, C. S., "Comparison of Calculated with Experimental Imbibition Relative Permeability," Trans. AIME **251**, 419-425 (1971).
[16] Standing, M. B., "Notes on Relative Permeability Relationships," unpublished notes distributed in Stanford University (1975), revised (1978).
[17] Ozgen, C., Chang, D. M., and HaiDorsen, H. H., "Simplified Oil-Water Relative Permeability Expressions Accounting for Hysteresis in the Imbibition Cycle," in *Reservoir Characterization II*, L. W. Lake, H. B. Carroll Jr., and T. C. Wesson, Eds., Academic Press (1986).
[18] Phelps, R. E., "Lithology-Dependent J-Functions and Relative Permeabilities," SPE paper 25661, SPE Middle East Oil Technical Conference, Bahrain, April 3-6 (1993).
[19] Pirson, S. J. , *Oil Reservoir Engineering*, p. 375-376, McGraw-Hill, 1958.
[20] Drake, L. C., and Ritter, H. L., "Pore-size Distribution in Porous Materials," Ind. Eng. Chem., Anal. Ed., **17**, pp. 782ff (1945).
[21] Hassler, G. L., and Brunner, E., "Measurement of Capillary Pressure in Small Core Samples," AIME Tech. Pub., p. 1917 (1945).
[22] Wardlaw, N. C., and Taylor, R. P., "Mercury Capillary Pressure Curves and the Interpretation of Pore Structure and Capillary Behavior in Reservoir Rocks," Bull. Canadian Pet. Geol. **24**, 225-262 (1976).
[23] Fatt, I. "The Network Model of Porous Media I, II, III," Trans. AIME **207**, 144-177 (1956).
[24] Jerauld, G. R., and Salter, S. L., "The Effect of Pore-Structure on Hysteresis in Relative Permeability and Capillary Pressure: Pore-Level Modeling," Trans. Porous Media **5**, 103-151 (1990).
[25] Heiba, A. A., Davis, H. T., and Scriven, L. E., "Statistical Network Theory of Three-Phase Relative Permeability," SPE/DOE paper 12690, Fourth Symposium on Enhanced Oil Recovery, Tulsa (1984).
[26] Parker, J. C., and Lenhard, R. J., "A Model for Hysteretic Constitutive Relations Governing Multiphase Flow, 1: Saturation-Pressure Relations," Water Resources Research **23,** 2187-2196 (1987).
[27] Donaldson, E. C., Thomas, R. D., and Lorenz, P. B., "Wettability Determination and Its Effect on Recovery Efficiency," SPEJ, March 13-20 (1969).
[28] Anderson, W. G., "Wettability Literature Survey - Part 2: Wettability Measurement," JPT, Nov. 1246-1262 (1986).
[29] Morrow, N. R., "Wettability and Its Effect on Oil Recovery," JPT, Dec. 1476-1484 (1990).
[30] Cook., N. G. W., "Geophysical and Transport Properties of Reservoir Rocks," Enhanced Oil Recovery Progress Review, No. 70., pp.52, DOE/BC (1992).
[31] Haring, R. E., and Greenkorn, R. A., "A Statistical Model of a Porous Medium with Nonuniform Pores," AIChE J. **16**, 477-483 (1970).
[32] Raza, S. H., Treiber, L. E., and Archer, D. L., "Wettability of Reservoir Rocks and Its Evaluation," Producers Monthly, April 2-7 (1968).
[33] Owens, W. W., and Archer, D. L., "The Effect of Rock Wettability on Oil-Water Relative Permeability Relationships," JPT, July 873-878 (1971).
[34] Kokkedee, J. A., and Boutkan, V. K., "Toward Measurement of Capillary Pressure and Relative Permeability at Representative Wettability," 1995 New Developments in Improved Oil Recovery, de Haan, H. J. (ed.), Geological Soc. Special Publication No. 84, p. 43-50.
[35] Honarpour, M. M., Huang, D. D., Payton, D. W., and Navarro, R., "Method and Apparatus for Measuring Properties of Core Samples including Heating and Pressurizing the Core Sample and Measuring the Dynamic and Static Capillary Pressure of Water in the Core Sample," US Patent 5,493,226, Feb. 20, 1996.
[36] Honarpour, M. M. and Huang, D. D. "Automated Microwave System for Simultaneous Measurements of Relative Permeability, Capillary Pressure, and Electrical Resistivity," SPE paper 30540, presented at the 1995 SPE Annual Meeting, Dallas. Reprinted in *SPE Journal*, September, 283-293 (1996).
[37] Maloney, D. and Brinkmeyer, A., "Three-Phase Permeabilities and Other Characteristics of 260-mD Fired Berea," NIPER-581, April 1992.